NIH Public Access
Author Manuscript
Bioorg Med Chem Lett. Author manuscript; available in PMC 2013 September 01.

Published in final edited form as:
Bioorg Med Chem Lett. 2012 September 1; 22(17): 5405–5409. doi:10.1016/j.bmcl.2012.07.044.

Near-infrared Fluorescent Divalent RGD Ligand for Integrin $\alpha_v\beta_3$-targeted Optical Imaging

Yunpeng Ye, **Walter Akers**, **Baogang Xu**, **Sharon Bloch**, **Charles Odonkor**, and **Samuel Achilefu**[*]
Department of Radiology, Optical Radiology Laboratory, Washington University School of Medicine, 4525 Scott Avenue, Saint Louis, MO 63108, USA.

Abstract

A new near-infrared fluorescent compound containing two cyclic RGD motifs, cypate-[c(RGDfK)]$_2$ (**1**), was synthesized based on a carbocyanine fluorophore bearing two carboxylic acid groups (cypate) for integrin $\alpha_v\beta_3$-targeting. Compared with its monovalent counterpart cypate-c(RGDfK) (**2**), **1** exhibited remarkable improvements in integrin $\alpha_v\beta_3$ binding affinity and tumor uptake in nude mice of A549. The results suggest that cypate-linked divalent ligands can serve as an important molecular platform for exploring receptor-targeted optical imaging and treatment of various diseases.

Keywords

integrin $\alpha_v\beta_3$; RGD peptide; divalent ligand; optical imaging; cypate

Among the family of 24 integrins, integrin $\alpha_v\beta_3$ has become an important target for cancer imaging and therapy. This is because the up-regulation of integrin $\alpha_v\beta_3$ in cancer and endothelial cells is implicated in the progression and metastasis of various tumors. Significant progress has been made in the discovery and development of integrin $\alpha_v\beta_3$-specific lactam-based cyclic RGD peptide analogs such as cilengitide and *c*(RGDfK) for cancer therapy, as well as targeted delivery of cancer imaging and therapeutic agents.[1–9] Nevertheless, it remains a great challenge to leverage such molecules into successful clinical applications due to the complexities of integrin signaling network in cancer cells, tumor microenvironments, and *in vivo* environments. For example, Reynolds et al. [10] reported that nanomolar concentrations of RGD-mimetic integrin $\alpha_v\beta_3$ and $\alpha_v\beta_5$ inhibitors can promote VEGF-mediated tumor angiogenesis and tumor growth in mice, which may seriously compromise the therapeutic efficacy of this class of compounds. Therefore, novel approaches for exploiting integrin $\alpha_v\beta_3$ targeting are still needed to improve cancer imaging, diagnosis, and therapy.

As one of the most versatile imaging modalities, optical imaging allows noninvasive, sensitive, and real time imaging of molecular interactions and related functions in cells,

© 2009 Elsevier Ltd. All rights reserved.

[*]Corresponding author. Fax: +1 314-747-5191, achilefus@mir.wustl.edu.

Publisher's Disclaimer: This is a PDF file of an unedited manuscript that has been accepted for publication. As a service to our customers we are providing this early version of the manuscript. The manuscript will undergo copyediting, typesetting, and review of the resulting proof before it is published in its final citable form. Please note that during the production process errors may be discovered which could affect the content, and all legal disclaimers that apply to the journal pertain.

Supplementary data
Supplementary data associated with this article can be found in the online version.

NIH-PA Author Manuscript
NIH-PA Author Manuscript
NIH-PA Author Manuscript

NIH-PA Author Manuscript

NIH-PA Author Manuscript

NIH-PA Author Manuscript

tissues, and *in vivo* systems. In particular, optical imaging serves as a powerful tool for bridging the wide gap between preclinical and clinical studies, facilitating the discovery of optimal integrin $\alpha_v\beta_3$-targeted molecules, and their subsequent translational studies. [11–14]

We previously reported a series of carbocyanine-based near-infrared (NIR) fluorescent probes for tumor-targeted optical imaging *in vivo*. [12, 13, 15–21] Noteworthy, a dicarboxylic acid-containing carbocyanine analog (cypate; Figure 1) can be used for facile conjugations of various bioactive molecules on solid support and in solution for molecular targeting of proteins expressed on plasma membrane, including integrin $\alpha_v\beta_3$ and somatostatin receptors. Cypate has also served as a robust scaffold for conveniently constructing novel divalent and multivalent fluorescent molecules for tumor-targeted optical imaging. In the present work, we aimed to synthesize and evaluate a novel integrin $\alpha_v\beta_3$-targeted divalent RGD ligand based on cypate for potential use in optical imaging of tumors. We hypothesized that **1** can simultaneously bind two adjacent $\alpha_v\beta_3$ integrins to enhance the $\alpha_v\beta_3$-binding affinity and tumor-targeting with improved imaging contrast compared with its monovalent counterpart **2**.

Initially, we prepared RGD peptide-dye conjugates from cypate and the non-protected cyclic peptide *c*(RGDfK) or *c*(RGDyK) via the reaction between two N-hydroxysuccinimidyl (NHS) esters of cypate and the amine group at the side chain of lysine residue as reported by others. [22, 23] However, we observed that the transformations of two carboxylic acid groups into the corresponding NHS esters were not complete despite using excessive amount of the coupling reagent DIC or EDCI. The additional EDCI could lead to activation of the carboxylic acid group at the side chain of Asp residue and related side reactions such as acylation of the free guanidine group in the Arg residues.[24] In a previous report, we demonstrated the successful synthesis of cypate-*c*(RGDfK) (**2**) by conjugating cypate with a protected cyclic RGD peptide, *c*[R(Pbf)GD(OBut)fK] **3**. Consequently, we chose to use the same strategy for the synthesis of the divalent compound **1** in this study.[19] The linear protected peptide H-D(OBut)-f-K(Dde)-R(Pbf)-G-OH was first assembled from H-Gly-2-chlorotrityl resin using the conventional Fmoc chemistry, followed by cleavage of the peptide from the resin with 1% TFA in DCM. The crude product was cyclized in the presence of PyBOP/HOBT/DIEA in dilute solution. The resulting cyclic protected peptide, *c*[R(Pbf)GD(OBut)fK(Dde)], was treated with 2% hydrazine in methanol to remove the Dde protecting group to form **3**. Cypate was synthesized from the benzoindo-acid and glutaconaldehyde via its pre-acetylation intermediate in a good yield as reported previously. [16, 18] Cypate (1 equiv) was conjugated with **3** (3 equiv) in the presence of EDCI (6 equiv) and HOBT (3 equiv) in DMF (Scheme 1). The crude product, cypate-{cyclo[R(Pbf)GD(OBut)fK(~)]}$_2$ (**4**), was de-protected with TFA and purified by semi-preparative reverse phase HPLC to afford the desired divalent RGD conjugate **1**. The compound was identified by analytical HPLC and LC-MS. As expected, **1**, **2**, and cypate showed similar UV-vis absorption and fluorescence emission spectra in 20% DMSO ($\lambda_{max/abs}$ and $\lambda_{max/em}$: 783 nm and 811 nm, respectively). [16]

The ligand-receptor binding is a complex process that can be affected by many factors, including the radioligand tracer, binding affinity, and concentration used as well as the receptor and new ligands tested. Most of the integrin $\alpha_v\beta_3$ binding assays have been based on competitive displacement against ^{125}I-labeled echistatin. Echistatin, an RGD-containing polypeptide isolated from viper venom, belongs to the disintegrin family of inhibitory proteins. It binds to integrin $\alpha_v\beta_3$ with high affinity, but competitive binding with linear and cyclic RGD peptides have been achieved. Previously, we determined the integrin $\alpha_v\beta_3$ binding affinities of some RGD compounds using ^{125}I-labeled echistatin tracer as reported by Kumar et al. [16, 25] We also used the integrin $\alpha_v\beta_3$-specific ligand *c*(RGDyK) labeled with ^{125}I at D-tyrosine (y) residue instead of ^{125}I-echistatin for the competitive integrin

NIH-PA Author Manuscript

NIH-PA Author Manuscript

NIH-PA Author Manuscript

$\alpha_v\beta_3$ binding assay. [17] The advantages of ^{125}I-c[RGDyK] over ^{125}I-echistatin include facile labeling, good quality control, and cost effectiveness.

In the present study, the radioactivity of c(RGDyK) peptide bound to integrin $\alpha_v\beta_3$ was determined with a gamma counter. Nonspecific binding of the tracer ^{125}I-c(RGDyK) was determined to be 5 to 10% of the total binding. The 50% inhibitory concentrations (IC_{50}) and affinity constant (Ki) were calculated by nonlinear regression analysis using the GraphPad Prism 4 data fitting software. The three RGD peptides, **1**, **2**, and *c*(RGDyK), were found to competitively inhibit the binding of ^{125}I-c(RGDyK) to $\alpha_v\beta_3$ in a concentration-dependent mode (Table 1). Compound **1** showed about 15 times stronger binding affinity than **2**, while both *c*(RGDyK) and **2** exhibited comparable IC_{50} values. In contrast, a scrambled analog, cypate-c(RGKDf), did not show significant inhibition compared with the other RGD compounds under the same condition (data not shown). The results further demonstrate the feasibility of using ^{125}I-*c*(RGDyK) as a tracer for integrin $\alpha_v\beta_3$ binding assays. Importantly, our study suggests that ^{125}I-c(RGDyK) is a reliable tracer for competitive binding assays of new compounds containing RGD structural motif with similar binding features and comparable binding affinity. Furthermore, ^{125}I-c(RGDyK) may serve as a sensitive method for studying some integrin $\alpha_v\beta_3$ ligands that could not compete favorably against ^{125}I-echistatin. We will further study the generality of ^{125}I-c(RGDyK) and compare it with ^{125}I-echistatin for studying integrin $\alpha_v\beta_3$-binding in future work.

NIR fluorescence microscopy was used to evaluate the compounds for integrin $\alpha_v\beta_3$-mediated cellular binding and uptake. This also allowed the imaging of **1**, **2**, and cypate in integrin $\alpha_v\beta_3$ positive A549 cells at different time points. The cell staining results are dependent on the incubation time (Figure 2). Compound **1** showed higher uptake than both **2** and cypate after 1 h of incubation. Nevertheless, their intracellular fluorescence reached comparable levels at 6 h, suggesting that the longer incubation time increased the non-specific uptake. These results also reflect the complex process of integrin $\alpha_v\beta_3$-mediated cellular internalization of the fluorescent divalent RGD compounds, which may be governed by multiple factors such as receptor binding, receptor expression level, and endocytosis, as well as the structures and related physicochemical properties of the tested compounds.

We further evaluated the subcellular distribution of **1**, **2**, and cypate by co-localization with MitoTracker Orange CM-TMRos® for the mitochondria (magenta) and DRAQ5 for the nucleus (blue). As shown in Figure 3, both **1** and **2** appear to have localized partially in the nucleus and the mitochondria. These results are consistent with previous reports by others. [26, 27]

To investigate integrin $\alpha_v\beta_3$ targeting and tumor localization *in vivo*, both **1** and **2** (100 μL, 60 μM) were intravenously injected by tail vein into nude mice bearing A549 tumor xenografts (5–7 mm diameter). Figure 4A shows the results of NIR fluorescence imaging (excitation and emission at 780nm and 830nm, respectively) at 1 h, 4 h, and 24 h post-injection. Compound **1** showed tumor localization in nude mice with good contrast between the tumor and non-target tissues at 4 h post-injection. In contrast, **2** had high accumulation in the liver and kidneys with low tumor uptake. Fluorescence intensity measurement shows that **1** had higher tumor/muscle ratio at 4 h and 8 h than **2** (Figure 4B). After euthanizing the animals at 24 h post-injection, the *ex vivo* organ analysis showed the relatively high uptake of **1** in the tumor and the liver compared with the kidneys, heart, and other tissues (Figure 4C and 4D). The results are in good agreement with the *in vivo* noninvasive optical imaging results.

Divalent and multivalent approaches have been widely studied in molecular discovery for improving the selectivity, specificity, and potency of receptor binding as well as the related

NIH-PA Author Manuscript

NIH-PA Author Manuscript

NIH-PA Author Manuscript

biological and pharmacological activities.[16, 28–32] Clearly, increased local concentration and divalent or multivalent interaction can enhance the integrin $\alpha_v\beta_3$ binding affinity of RGD compounds. Various divalent and multivalent RGD peptides for integrin $\alpha_v\beta_3$-targeted imaging such as $^{18>}$F-FPPRGD2 and some fluorescent labeled RGD compounds have also been reported for tumor targeted imaging, therapy, and drug delivery. [14, 16, 26, 32–37] Especially, it is important to have the suitable linkage between two RGD motifs that can span the two neighboring integrin $\alpha_v\beta_3$ sites for simultaneous binding. As shown above, **1** represents a new type of NIR fluorescent divalent ligands using cypate as both linker and probe. Unlike other flexible linkers, the cypate motif consists of ploymethines and benzoindoline rings, which might help to pre-organize the divalent RGD ligand for simultaneous binding of two adjacent $\alpha_v\beta_3$ integrins with decreased binding entropy and enhanced stability of the resulting ligand-receptor complex.

By comparing with **2** and cypate, the significant improvement of **1** in tumor localization suggests the enhanced integrin $\alpha_v\beta_3$-targeting for tumor optical imaging. The results also support our hypothesis that the divalent compound can simultaneously bind to two adjacent integrin $\alpha_v\beta_3$ proteins and exhibit synergistic effects on receptor- and tumor-targeting. Furthermore, the linker of a divalent ligand plays an important role in achieving significant synergistic effects. [4, 31] The 27-atom length between the two RGD motifs of **1** may be sufficiently long to span two adjacent $\alpha_v\beta_3$ for simultaneous binding, leading to improvement in the integrin $\alpha_v\beta_3$ binding affinity and related tumor targeting (Figure 5). Therefore, compound **1** could serve as a prototype for constructing and optimizing novel integrin $\alpha_v\beta_3$-targeted compounds for the early diagnosis and targeted therapy of tumors.

There was high accumulation of **1** in the liver (Figure 4), which suggests its clearance from circulation through the reticuloendothelial system (RES). The strong NIR fluorescence in the mice over 24 h post-injection of **1** demonstrates the *in vivo* stability of **1** and its possible metabolites. As reported previously, NIR fluorescent IRDye800-RGD conjugates showed rapid clearance via the kidneys, and low tumor fluorescence ensued at 4 h post injection. [38] These differences illustrate the important roles of the dye motif and the related hydrophilicity in the dynamics of divalent molecular imaging probes. These results also provide an insight into further structural modification of the cypate motif to minimize non-specific binding so as to enhance integrin $\alpha_v\beta_3$ and tumor-selective targeting.

Noteworthy, the modular approach we have used for synthesis of **1** allows for convenient preparation of such divalent conjugates in solution and / or on solid support. A vast array of molecules with distinct chemical and biological characteristics can be obtained by varying the peptide, linker, and cypate to elucidate the structure-activity relationship and mechanism of molecular targeting. In addition to integrin $\alpha_v\beta_3$, various cancer cell surface receptors such as somatostatin, growth factor, and steroid receptors associated with cancer initiation and progression have been reported. Therefore, cypate can serve as a unique fluorescent linker for conveniently constructing diverse divalent ligands to explore ligand-receptor and receptor-receptor interactions by optical imaging.

In summary, we have synthesized and evaluated a novel fluorescent divalent c(RGDfK) analog **1** based on cypate for integrin $\alpha_v\beta_3$ targeted optical imaging of tumors. The promising *in vitro* and *in vivo* data suggest that fluorescent divalent ligands of this type serve as an important strategy for exploring receptor-targeted optical imaging and provide insight into a better understanding of ligand design principles, structural optimization, and mechanism of action for specific receptor-targeting.

NIH-PA Author Manuscript

NIH-PA Author Manuscript

NIH-PA Author Manuscript

Supplementary Material

Refer to Web version on PubMed Central for supplementary material.

Acknowledgments

This work was supported in part by the US National Institutes of Health grants. This study is based upon work supported in part by the NIH grants NCI R01 CA109754, R33 CA123537, R01 EB008111, and R01 EB007276.

References and notes

1. Xiong JP, Stehle T, Diefenbach B, Zhang R, Dunker R, Scott DL, Joachimiak A, Goodman SL, Arnaout MA. Science. 2001; 294:339. [PubMed: 11546839]
2. Tucker GC. Curr Opin Investig Drugs. 2003; 4:722.
3. Chen X, Sievers E, Hou Y, Park R, Tohme M, Bart R, Bremner R, Bading JR, Conti PS. Neoplasia. 2005; 7:271. [PubMed: 15799827]
4. Liu S. Mol Pharm. 2006; 3:472. [PubMed: 17009846]
5. Hsu AR, Veeravagu A, Cai W, Hou LC, Tse V, Chen X. Recent Pat Anticancer Drug Discov. 2007; 2:143. [PubMed: 18221059]
6. Schottelius M, Laufer B, Kessler H, Wester HJ. Acc Chem Res. 2009; 42:969. [PubMed: 19489579]
7. Zannetti A, Del Vecchio S, Iommelli F, Del Gatto A, De Luca S, Zaccaro L, Papaccioli A, Sommella J, Panico M, Speranza A, Grieco P, Novellino E, Saviano M, Pedone C, Salvatore M. Clin Cancer Res. 2009; 15:5224. [PubMed: 19671851]
8. Temming K, Schiffelers RM, Molema G, Kok RJ. Drug Resist Updat. 2005; 8:381. [PubMed: 16309948]
9. Benezra M, Penate-Medina O, Zanzonico PB, Schaer D, Ow H, Burns A, DeStanchina E, Longo V, Herz E, Iyer S, Wolchok J, Larson SM, Wiesner U, Bradbury MS. The Journal of clinical investigation. 2011; 121:2768. [PubMed: 21670497]
10. Reynolds AR, Hart IR, Watson AR, Welti JC, Silva RG, Robinson SD, Da Violante G, Gourlaouen M, Salih M, Jones MC, Jones DT, Saunders G, Kostourou V, Perron-Sierra F, Norman JC, Tucker GC, Hodivala-Dilke KM. Nat Med. 2009; 15:392. [PubMed: 19305413]
11. Achilefu S. Technol Cancer Res Treat. 2004; 3:393. [PubMed: 15270591]
12. Achilefu S, Dorshow RB, Bugaj JE, Rajagopalan R. Invest Radiol. 2000; 35:479. [PubMed: 10946975]
13. Bugaj JE, Achilefu S, Dorshow RB, Rajagopalan R. J Biomed Opt. 2001; 6:122. [PubMed: 11375721]
14. Ye Y, Chen X. Theranostics. 1:102. [PubMed: 21546996]
15. Achilefu S, Bloch S, Markiewicz MA, Zhong T, Ye Y, Dorshow RB, Chance B, Liang K. Proc Natl Acad Sci U S A. 2005; 102:7976. [PubMed: 15911748]
16. Ye Y, Bloch S, Xu B, Achilefu S. J Med Chem. 2006; 49:2268. [PubMed: 16570923]
17. Edwards WB, Akers WJ, Ye Y, Cheney PP, Bloch S, Xu B, Laforest R, Achilefu S. Mol Imaging. 2009; 8:101. [PubMed: 19397855]
18. Ye Y, Bloch S, Kao J, Achilefu S. Bioconjug Chem. 2005; 16:51. [PubMed: 15656575]
19. Ye Y, Bloch S, Xu B, Achilefu S. Bioconjug Chem. 2008; 19:225. [PubMed: 18038965]
20. Pu Y, Wang WB, Tang GC, Zeng F, Achilefu S, Vitenson JH, Sawczuk I, Peters S, Lombardo JM, Alfano RR. Technol Cancer Res Treat. 2005; 4:429. [PubMed: 16029061]
21. Ye Y, Xu B, Nikiforovich GV, Bloch S, Achilefu S. Bioorganic & medicinal chemistry letters. 2011; 21:2116. [PubMed: 21349709]
22. Chen X, Park R, Tohme M, Shahinian AH, Bading JR, Conti PS. Bioconjug Chem. 2004; 15:41. [PubMed: 14733582]
23. Chen X, Plasencia C, Hou Y, Neamati N. J Med Chem. 2005; 48:1098. [PubMed: 15715477]
24. Weiss S, Keller M, Bernhardt G, Buschauer A, Konig B. Bioorg Med Chem. 18:6292. [PubMed: 20688523]

NIH-PA Author Manuscript

NIH-PA Author Manuscript

NIH-PA Author Manuscript

25. Kumar CC, Nie H, Rogers CP, Malkowski M, Maxwell E, Catino JJ, Armstrong L. J Pharmacol Exp Ther. 1997; 283:843. [PubMed: 9353406]
26. Borgne-Sanchez A, Dupont S, Langonne A, Baux L, Lecoeur H, Chauvier D, Lassalle M, Deas O, Briere JJ, Brabant M, Roux P, Pechoux C, Briand JP, Hoebeke J, Deniaud A, Brenner C, Rustin P, Edelman L, Rebouillat D, Jacotot E. Cell Death Differ. 2007; 14:422. [PubMed: 16888644]
27. Werner E, Werb Z. J Cell Biol. 2002; 158:357. [PubMed: 12119354]
28. Vaidyanath A, Hashizume T, Nagaoka T, Takeyasu N, Satoh H, Chen L, Wang J, Kasai T, Kudoh T, Satoh A, Fu L, Seno M. J Cell Mol Med. 15:2525. [PubMed: 21323863]
29. Xu L, Vagner J, Alleti R, Rao V, Jagadish B, Morse DL, Hruby VJ, Gillies RJ, Mash EA. Bioorganic & medicinal chemistry letters. 20:2489. [PubMed: 20304640]
30. Knor S, Sato S, Huber T, Morgenstern A, Bruchertseifer F, Schmitt M, Kessler H, Senekowitsch-Schmidtke R, Magdolen V, Seidl C. Eur J Nucl Med Mol Imaging. 2008; 35:53. [PubMed: 17891393]
31. Shewmake TA, Solis FJ, Gillies RJ, Caplan MR. Biomacromolecules. 2008; 9:3057. [PubMed: 18828631]
32. Ryppa C, Mann-Steinberg H, Biniossek ML, Satchi-Fainaro R, Kratz F. Int J Pharm. 2009; 368:89. [PubMed: 18992308]
33. Liu Z, Liu S, Wang F, Chen X. Eur J Nucl Med Mol Imaging. 2009; 36:1296. [PubMed: 19296102]
34. Shi J, Kim YS, Zhai S, Liu Z, Chen X, Liu S. Bioconjug Chem. 2009; 20:750. [PubMed: 19320477]
35. Aaron J, Nitin N, Travis K, Kumar S, Collier T, Park SY, Jose-Yacaman M, Coghlan L, Follen M, Richards-Kortum R, Sokolov K. J Biomed Opt. 2007; 12:034007. [PubMed: 17614715]
36. Jin ZH, Furukawa T, Waki A, Akaji K, Coll JL, Saga T, Fujibayashi Y. Biol Pharm Bull. 33:370. [PubMed: 20190395]
37. Cheng Z, Wu Y, Xiong Z, Gambhir SS, Chen X. Bioconjug Chem. 2005; 16:1433. [PubMed: 16287239]
38. Ye Y, Zhu L, Ma Y, Niu G, Chen X. Bioorganic & medicinal chemistry letters. 21:1146. [PubMed: 21251820]

NIH-PA Author Manuscript
NIH-PA Author Manuscript
NIH-PA Author Manuscript

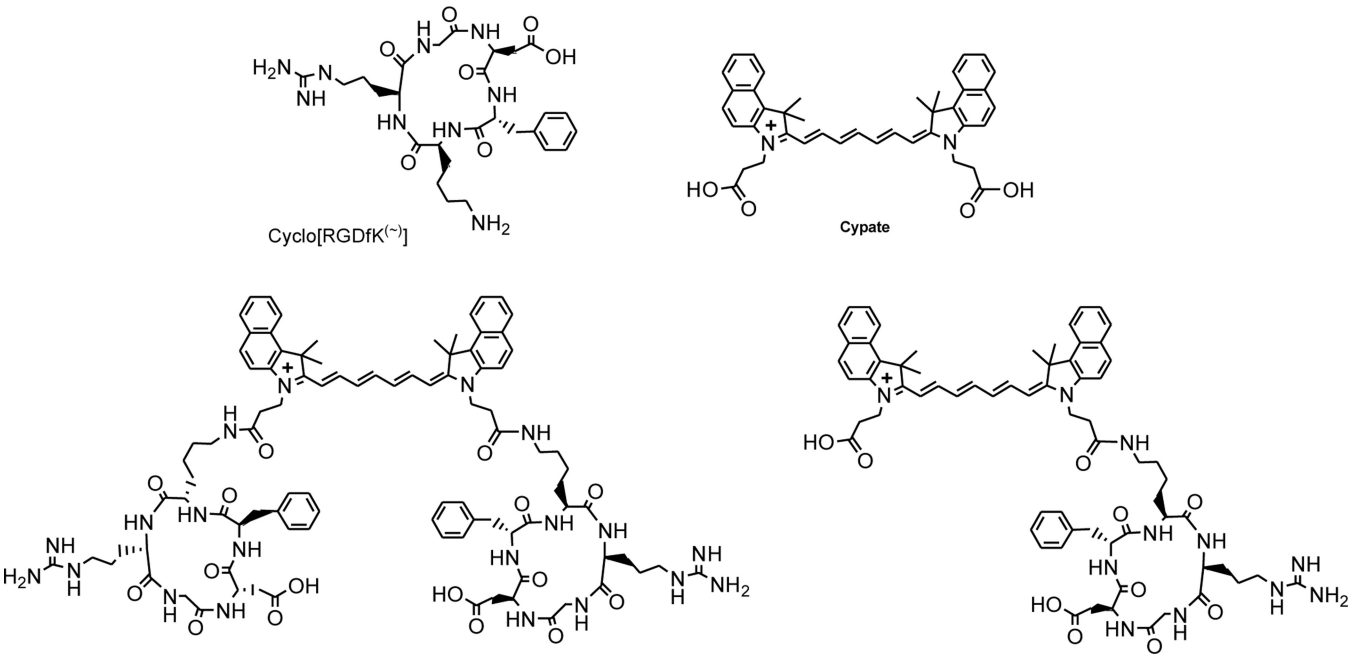

Figure 1.
Near-infrared fluorescent cypate and its RGD conjugates.

NIH-PA Author Manuscript

NIH-PA Author Manuscript

NIH-PA Author Manuscript

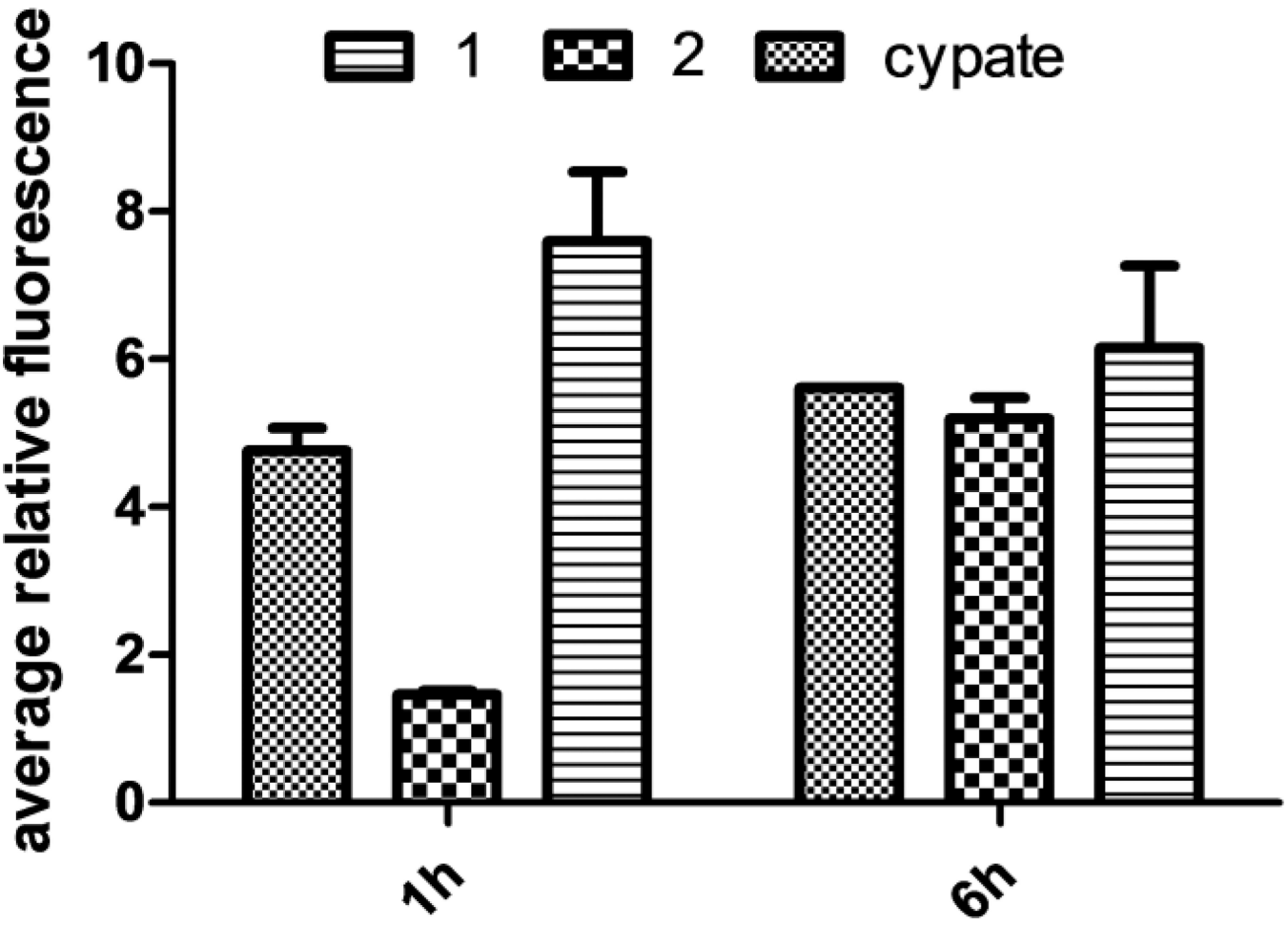

Figure 2.
Binding and internalization of **1**, **2**, and cypate in A549 cells at different time points.

NIH-PA Author Manuscript

NIH-PA Author Manuscript

NIH-PA Author Manuscript

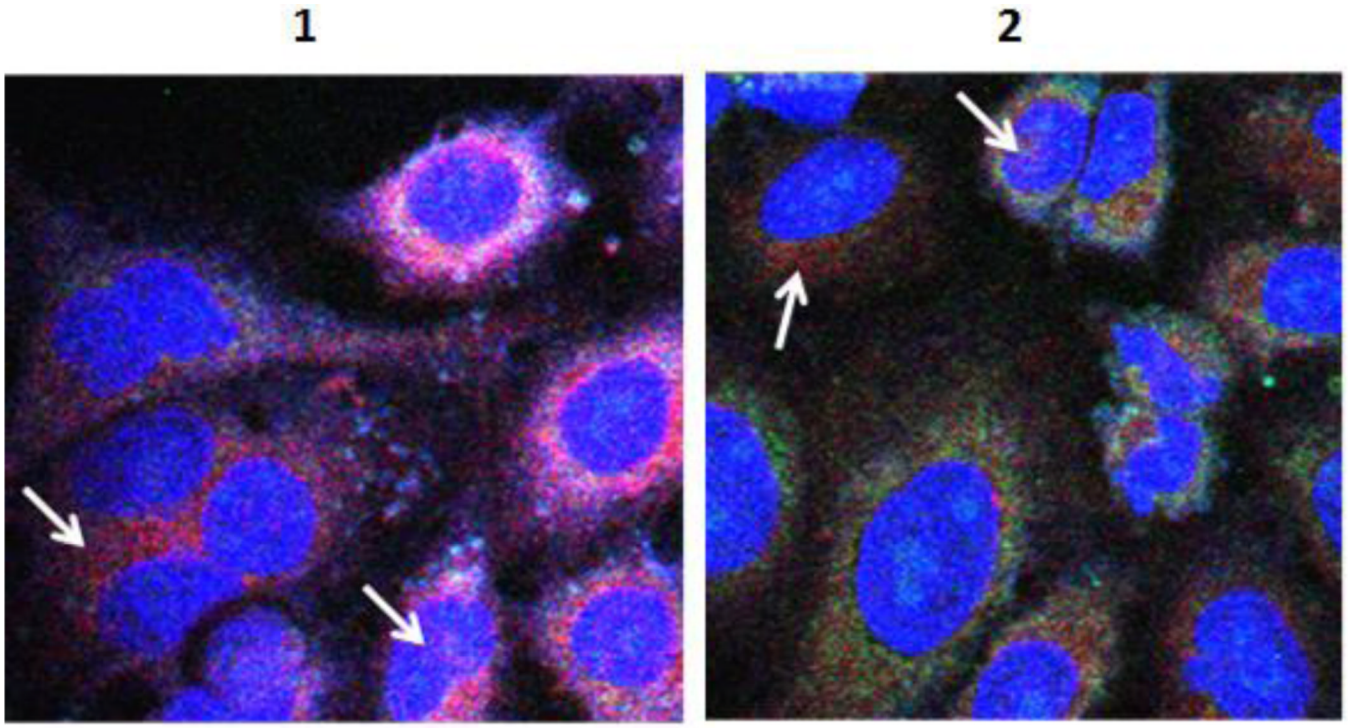

Figure 3.

Subcellular distribution of **1** and **2** at 16 h of incubation. Fluorescent probes were excited (at 488 nm, 633 nm and 755 nm) and two-dimensional confocal images acquired by scanning a field at 2 μs per pixel. Each image shows overlay of nuclear stain (blue), mitochondrial stain (green) and cypate (red). Arrows point to cypate fluorescence indicative of the presence of the compound in the marked region.

NIH-PA Author Manuscript
NIH-PA Author Manuscript
NIH-PA Author Manuscript

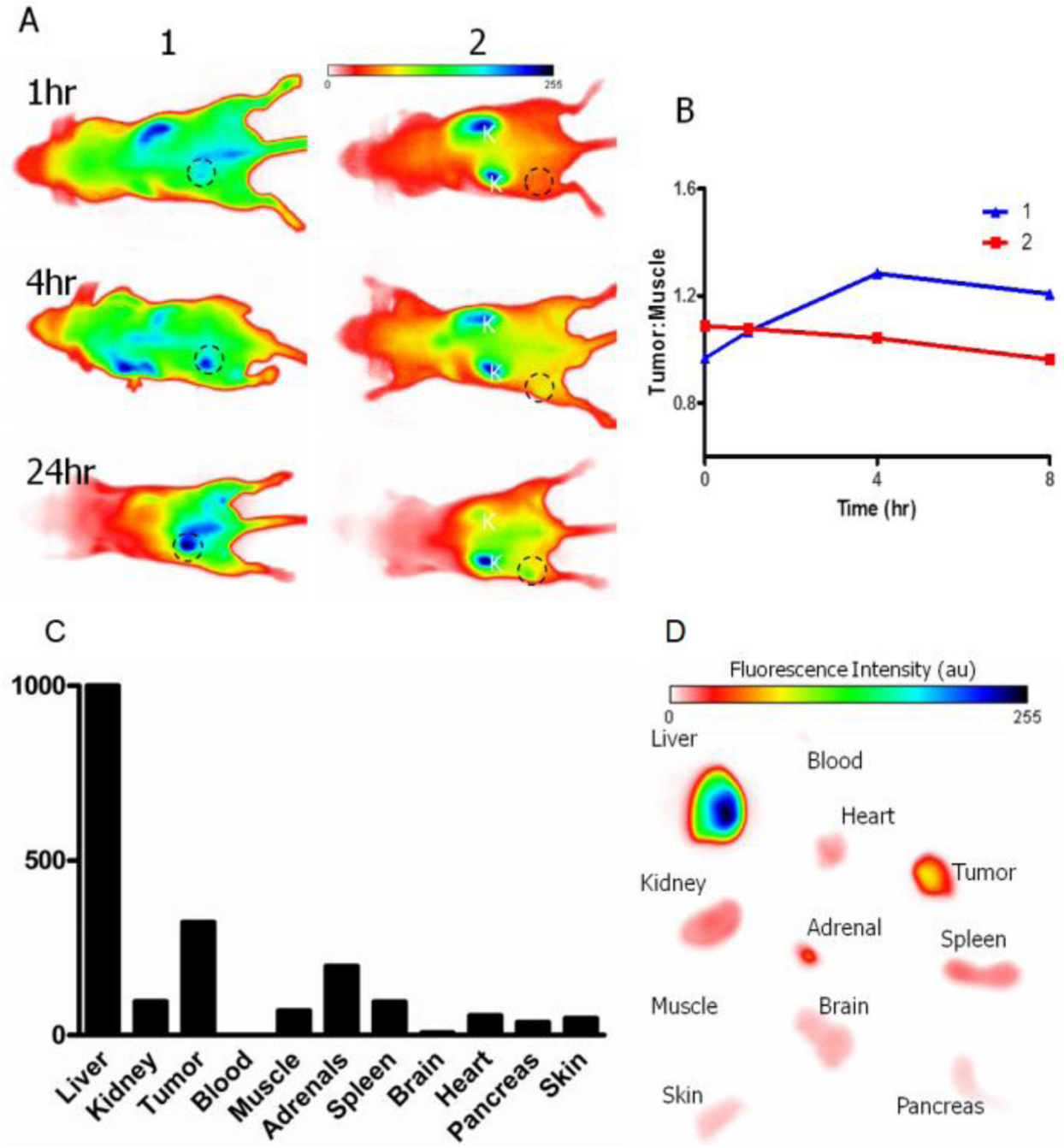

Figure 4.

Optical imaging of **1** and **2** in mice. (A) *In vivo* optical imaging of tumors (circled areas) at 1, 4, and 24 h post –injection; (B) time-dependent tumor uptake; (C) *ex vivo* biodistribution of fluorescence at 24 h post-injection; and (D) *ex vivo* fluorescence imaging of representative organs.

NIH-PA Author Manuscript
NIH-PA Author Manuscript
NIH-PA Author Manuscript

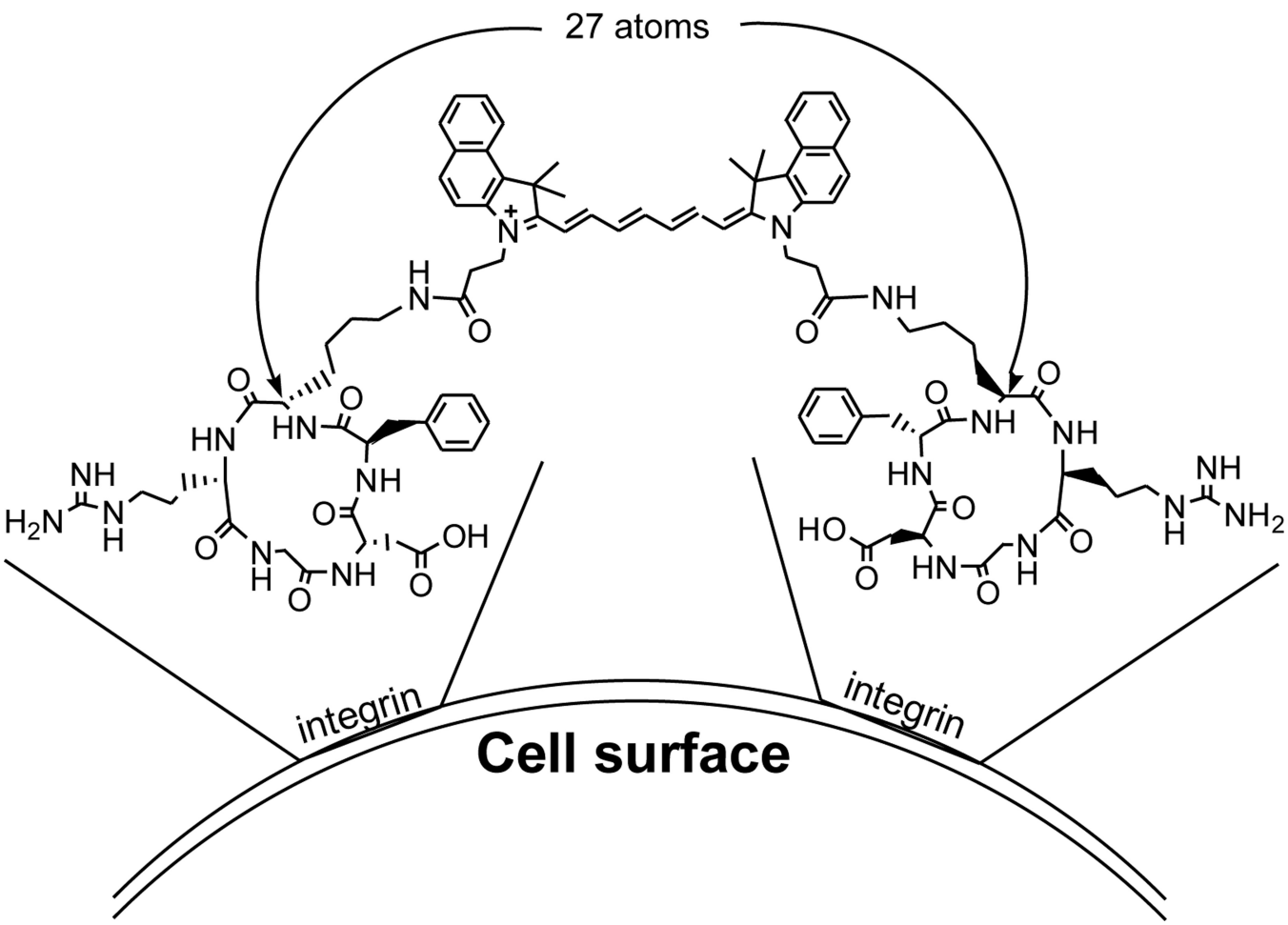

Figure 5.
The two RGD motifs linked by cypate for simultaneous binding of two $\alpha_v\beta_3$ integrins.

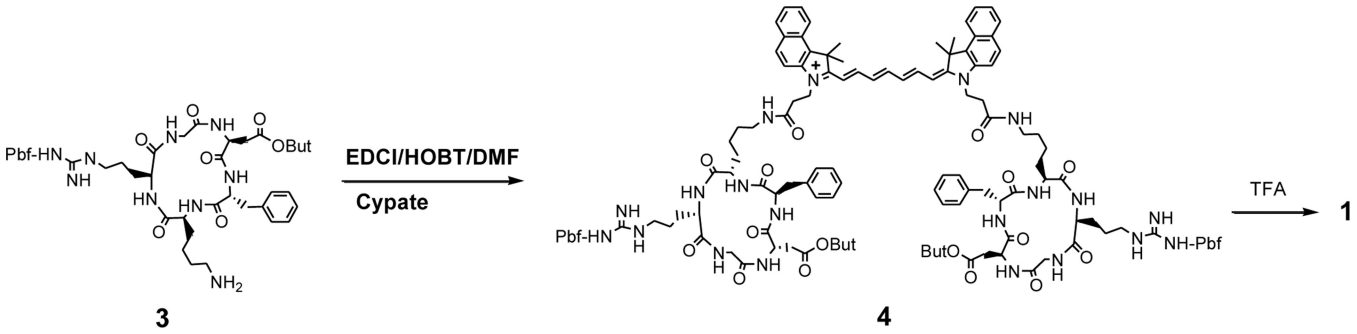

Scheme 1.
Synthesis of the divalent RGD-cypate conjugates **1**.

NIH-PA Author Manuscript NIH-PA Author Manuscript NIH-PA Author Manuscript

NIH-PA Author Manuscript

NIH-PA Author Manuscript

NIH-PA Author Manuscript

Table 1

The integrin $\alpha_v\beta_3$ binding of 1 and 2 traced by ^{125}I-*c*(RGDyK).

Compound	IC_{50} (nM, Mean ± SD)	Ki (Mean ± SD)	R^2
1	0.281 ± 0.009	0.043 ± 0.015	0.957
2	4.305 ± 0.056	0.663 ± 0.086	0.9874
c(RGDyK)	3.52 ± 0.354	2.27 ± 0.228	0.9957